Fermilab Proton Driver Neutrino Scattering Physics Working Group Report

Convenors
Jorge G. Morfín*, Ronald Ransome† and Rex Tayloe‡

February 8, 2005

1 Introduction

The Fermilab proton driver, with high-intensity neutrino and antineutrino beams produced from 8 and 120 GeV protons, will offer a unique opportunity to explore neutrino scattering processes with unprecedented precision. While there will have been significant progress made in this area with current and currently planned experiments, existing beams will lack the intensity needed to make the precision measurements required for complete understanding of the physics.

The pre-proton-driver experiments will provide measurements of charged-current (CC) and neutral-current (NC) (quasi)elastic scattering and CC and NC production of pions and strange particles on nuclear targets. It will remain for the proton-driver to make high-precision measurements of these processes with antineutrino beams and with nucleon targets. Neutrino-electron elastic scattering requires a proton-driver class neutrino beam. For this program of measurements, high intensity, low duty-factor neutrino and antineutrino beams from both 8 and 120 GeV proton sources are required. The details of the physics case for this is made in the following sections.

The 8 and 120 GeV beams are complementary and both are required for the full physics program. The 8 GeV beam will provide a low-energy narrow-band beam to allow for measurements of reaction channels where it is crucial to minimize backgrounds resulting from high-energy component of the beam. The 120 GeV beam will provide higher rates from low cross section processes due to the higher energy component of the beam and can explore the deep-inelastic scattering regime.

It is assumed in the following sections, that these current and near-future experiments will have completed relevant measurements by the time of start-up of the proton driver:

- Auxiliary experiments to predict the neutrino flux such as HARP, BNL E910, and MIPP;
- Jefferson lab high precision elastic scattering experiments for precision determination of the vector form factors;
- The K2K suite of near detector experiments including the SCIBAR experiment;
- The MiniBooNe experiment;
- The MINERνA experiment running parasitically to MINOS;

*Fermilab
†Rutgers University
‡Indiana University

- The proposed FINeSSE experiment running on an $E_\nu \approx 1$ GeV neutrino beamline; and
- T2K-I, although details of a neutrino scattering detector are not yet known.

A review of what we expect to be the state of knowledge of neutrino scattering physics and what will still be awaiting experimentation is summarized below.

2 Neutrino Scattering Physics with a High-Intensity 8 GeV Proton Driver

2.1 Introduction

A program of neutrino scattering physics using a neutrino beam from a high-intensity 8 GeV proton source is an important component of the physics case for a proton driver at FNAL. This program would use neutrino and antineutrino beams with a mean energy of approximately 1 GeV to make high-accuracy cross section measurements needed for a precise determination of neutrino oscillation parameters. In addition, measurements required to obtain a deeper understanding of the structure of the nucleon and the properties of neutrinos could be performed. This program would be complementary to measurements carried out using a neutrino beam from a 120 GeV proton source and would provide some results unobtainable from the higher energy beam.

2.2 Physics with an 8 GeV proton-driver neutrino beam

The available data on neutrino scattering in the $E_\nu \approx 1$ GeV region, predominantly from bubble chamber experiments of 2-3 decades ago, is quite sparse. Currently running or proposed experiments such as the K2K near detectors [1], MiniBooNE [2], T2K near detectors, MINERνA [4], and FINeSSE [5] will have improved this situation substantially with measurements of neutrino scattering on nuclear targets, including carbon and oxygen. These data will provide much needed cross sections for the large neutrino oscillation experiments and will lead to greater understanding of the nuclear physics behind these processes. However, the intensities provided by the neutrino sources used by these experiments are not high enough for precision measurements with antineutrinos and neutrinos on nucleon targets (H_2 and D_2). These measurements will be the next step required to elucidate the physics accessible with neutrinos. For this, a 2 MW proton-driver providing high-intensity $\approx$1 GeV neutrino and antineutrino beams to fine-grained, modest-sized, near-detector experiments is required.

It is important to understand the physics of neutrino scattering in the 1-10 GeV energy range. The rates of neutrino scattering processes need to be measured in dedicated experiments in order to make precise neutrino oscillation measurements. Robust calculations of these rates require a complete understanding of the physics behind the scattering. In addition, the physics of neutrino scattering is itself an important topic to pursue. The structure of the nucleon is still not adequately known and is an area of intense study at labs around the world. Neutrinos are a sensitive probe of this physics.

The neutrino scattering processes of interest are:

- charged-current (CC) quasielastic scattering,
- neutral-current (NC) elastic scattering,
- resonance and coherent production of pions in charged- and neutral-current scattering,
- neutrino production of strange particles, and
- neutrino-electron elastic scattering.

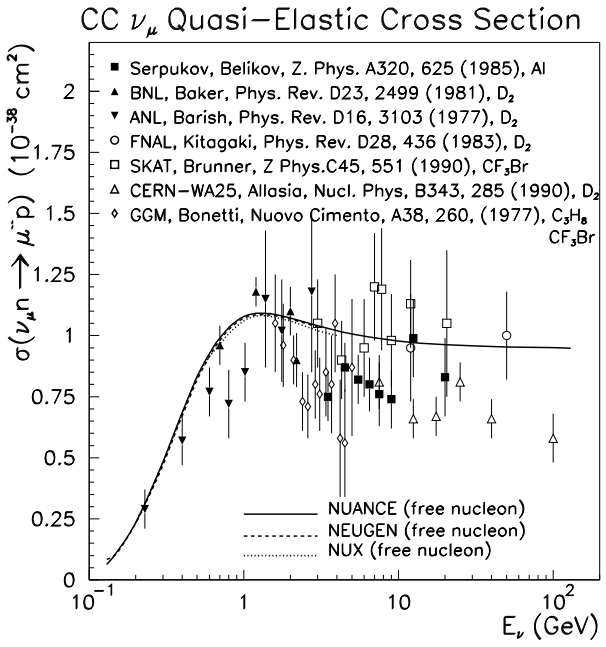

Figure 1: Cross section per nucleon for CC $\nu_m u$ quasielastic scattering. The curves are from several neutrino event generators.

In the following subsections we elaborate on the physics interest of each of these channels, the current state of the data, what will likely not be known at the time of the proton driver turn-on, and what experiments will require the proton driver.

2.2.1 Charged-Current quasielastic scattering

The charged-current quasielastic process for both neutrinos and antineutrinos ($\nu n \rightarrow \mu^- p$, $\bar{\nu} p \rightarrow \mu^+ n$) allows for high-accuracy tests of nucleon structure and better understanding of the effects of the binding of nucleons in the nucleus.

At 1 GeV neutrino energy, this process dominates the neutrino interaction rates. Previous data is mostly from bubble experiments measuring scattering on light targets such as D_2. The largest data samples contain $\approx$ 2500 events for neutrino scattering on D_2 and $\approx$ 800 events for antineutrino scattering on a target containing a mixture of C, H, F, and Br. These data are shown in Figures 1 and 2.

Currently running experiments such as K2K and MiniBooNE have already collected an order of magnitude more data than previous experiments, but using neutrinos on carbon and oxygen targets. The proposed FINeSSE experiment will precisely measure the charged-current quasielastic channel using a carbon target in the $E_\nu \approx 1$ GeV range; the T2K near detector will do the same using an oxygen target. The proposed MINERνA experiment will make this measurement at higher energies. However, a very intense $E_\nu \approx 1$ neutrino source, such as the proposed proton driver beam, will be required to precisely measure neutrino quasielastic scattering on nucleon targets (H_2 and D_2) and to precisely measure antineutrino quasielastic scattering on nucleon and nuclear targets.

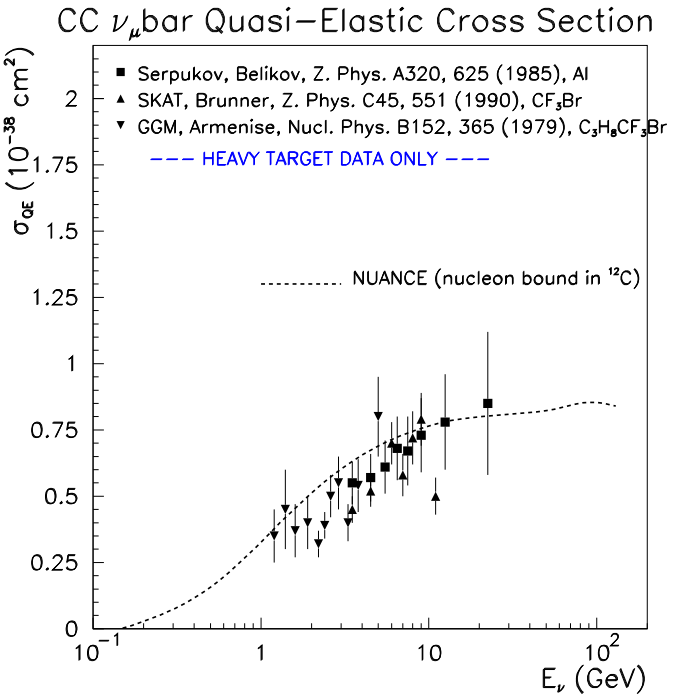

Figure 2: Cross section per nucleon for CC $\bar{\nu}_m u$ quasielastic scattering. The curve is from the NUANCE neutrino event generator.

2.2.2 Neutral-Current elastic scattering

The neutral-current elastic scattering of neutrinos and antineutrinos on nucleons ($\nu N \rightarrow \nu N$, $\bar{\nu} N \rightarrow \bar{\nu} N$) provides information about the spin structure of the nucleon. These scattering processes are sensitive to the isoscalar spin structure of the nucleon such as would result from the presence of strange quarks. This strange quark contribution, Δs, has been measured to be ≈ -0.1 in deep-inelastic (DIS) polarized lepton experiments [6]. However, the procedure to extract Δs from DIS data is subject to model dependence and relies on the assumption of SU(3) symmetry. A precise measurement of neutral-current elastic scattering would provide a direct measurement of Δs that is insensitive to theoretical assumptions.

The best measurement to date of NC elastic scattering comes from Brookhaven experiment BNL E734 [7], which ran approximately 20 years ago. They gathered a data set of ≈ 1000 events for both neutrino and antineutrino scattering in a liquid scintillator target. This data is consistent with the interpretation of the data from DIS scattering (namely $\Delta s \approx -0.1$), however, the precision is lacking due to the limited event size and relatively large Q^2 of the measurement.

The proposed FINeSSE experiment is designed to make an accurate measurement of Δs by measuring the ratio of NC elastic scattering to CC quasielastic scattering. This allows for the extraction of Δs with small uncertainties as many systematic uncertainties are reduced substantially in the ratio (e.g. uncertainty in neutrino flux). However, this measurement will be made in liquid scintillator and the scattering will take place predominantly on nucleons bound in carbon. In addition, a measurement of NC elastic scattering with both neutrinos *and antineutrinos* would further reduce systematics due to uncertainties in proton form factors.

The ultimate goal of a program of measurements would be to measure NC elastic scattering with both neutrinos and antineutrinos, with large event samples, on *nucleon* targets (H_2 and D_2). The intense neutrino flux required for these measurements would be possible only at a location near the source of an intense neutrino beam such as that from the proton driver.

2.2.3 Resonant and coherent production of pions

The study of resonant production of pions in CC and NC neutrino and antineutrino scattering provides important information about the resonance structure of the nucleon. A study of resonance structure of the nucleon via the weak interaction and a comparison of information obtained with neutrinos to that from antineutrinos, would allow for strong tests of our understanding of non-perturbative QCD. In particular, an extraction of the $N\Delta$ form factor tests nucleon models where the pion is an important component in the nucleon degrees of freedom. How to bring this model of the nucleon together with nucleon models consisting of gluons and quarks is a major question in nuclear physics.

In the coherent pion production process, the scattering occurs from the nucleus as a whole at low-Q^2. At $Q^2 = 0$ the cross section may be written in a simple form due to the PCAC hypothesis [8]. However, the extension to larger Q^2 is not well-understood and there are significant variations between models.

Existing data on these channels predominantly comes from older bubble chamber experiments with small data samples. There are several fairly large disagreements between different experiments and between experiment and current models. The currently running MiniBooNE and K2K experiments will provide better data. However, data from antineutrinos and nucleon targets would be needed for a complete data set.

2.2.4 Neutrino Production of Strange Particles

The production of strange mesons and hyperons in neutrino NC and CC processes such as $\nu_\mu n \to \mu^- K^+ \Lambda^0$ and $\nu_\mu p \to \nu_\mu K^+ \Lambda^0$ is important as it provides input to the few theoretical models of neutrino-induced strangeness production. In addition to the physics insight gained, neutrino induced strangeness production is a significant background in searches for proton decay based on SUSY-inspired proton decay mode $p \to \nu \Lambda K^+$.

The existing experimental data on these channels consists of only a handful of events from bubble chamber experiments. There are plans to measure these reactions from the existing K2K and the proposed MINERvA experiments. MINERvA will collect a large sample ($\approx 10,000$) of $\nu_\mu n \to \mu^- K^+ \Lambda^0$ events. However, it will be necessary to measure with antineutrinos requiring a more intense source to provide the needed input for strangeness production models [9].

2.2.5 Neutrino electron elastic scattering

The neutrino-electron elastic scattering process ($\nu e \to \nu e$) is well-known theoretically in the electroweak model. Because of this, it is a prime candidate for searches into new physics. With sufficient statistics and a well-known neutrino beam, a precision measurement of $\sin^2\theta_W$ would be possible. However, that requires an absolute measurement and is not likely possible, even with a proton-driver class neutrino beam. However, measurements which rely on the well-known energy-dependent shape of the cross section for this process could conduct a profitable search for new physics. This is the case for a measurement of the neutrino magnetic moment.

In the minimal standard model, neutrinos are massless and have no magnetic moment. However, if neutrinos do have mass as indicated in recent data, they may acquire a magnetic moment via radiative corrections. In this scenario, with $m_\nu = 1$ eV, the magnetic moment would be $\approx 3 \times 10^{-19} \mu_B$ where $\mu_B = e/2m_e$ is the Bohr magneton. This value is too small to be detected or to affect astrophysical processes. However, in other extensions to the standard model, the neutrino may acquire a magnetic moment on the order of $1 \times 10^{-11} \mu_B$ which is only an order of magnitude lower than present limits.

The current best limit on the muon neutrino magnetic moment is $\mu_{\nu_\mu} \leq 6.8 \times 10^{-10} \mu_B$ from LSND $\nu_\mu e$ elastic scattering [10]. This limit may be substantially reduced, perhaps to the level of some theoretical predictions, by precisely measuring the elastic scattering rate as a function of electron recoil energy. An electromagnetic contribution (from the magnetic moment) to the cross section will show up as an increase in event rate at the lower electron recoil energies as is shown in Figure 3.

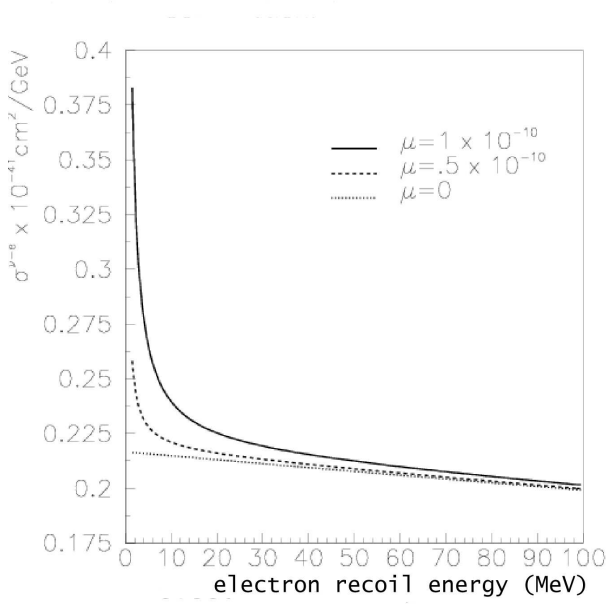

Figure 3: Differential cross section versus electron recoil kinetic energy, T, for $\nu e \to \nu e$ events. The electroweak contribution is linear in T (bottommost line), while contributions from nonzero neutrino magnetic moments yield sharp rises at low T.

To do this experiment, a precise tracking detector with a low electron energy threshold at a near location on an intense neutrino beam is required. This would be possible on the low-energy neutrino line of the proton driver. Depending on the energy threshold achievable, a gain of 10-30 over the LSND measurement is possible.

2.3 Beam Requirements

In order to make the measurements outlined above, high-intensity neutrino and antineutrino beams of mean energy ≈ 1 GeV are required. It is important that this beam have no high-energy tail (above ≈ 2 GeV) so that backgrounds from multipion and deep-inelastic scattering processes do not overwhelm the signal reactions of interest. The energy distribution of the booster neutrino beam, currently in operation at Fermilab, is ideal for these studies, as shown in Fig. 4. A proton-driver beam that uses a similar horn-focusing system would satisfy the beam requirements.

It is imperative to have the highest intensity available in order to do this physics, especially for antineutrinos where the neutrino production and reaction rate is substantially reduced. For this reason, the full 2 MW 8 GeV linac scenario is strongly encouraged. This would allow for the complete physics program, using neutrino and antineutrinos on nuclear targets.

It is also important for the neutrino beam to have a very low duty-factor, as is possible with a bunching scheme utilizing a storage ring. Beam-unrelated cosmic-ray-induced backgrounds increase with the duty-factor of the delivered beam. Many of the neutrino measurements discussed above require low backgrounds for low energy final states (e.g. NC elastic scattering and neutrino-electron elastic scattering). These measurements would be limited with a high duty-factor neutrino beam.

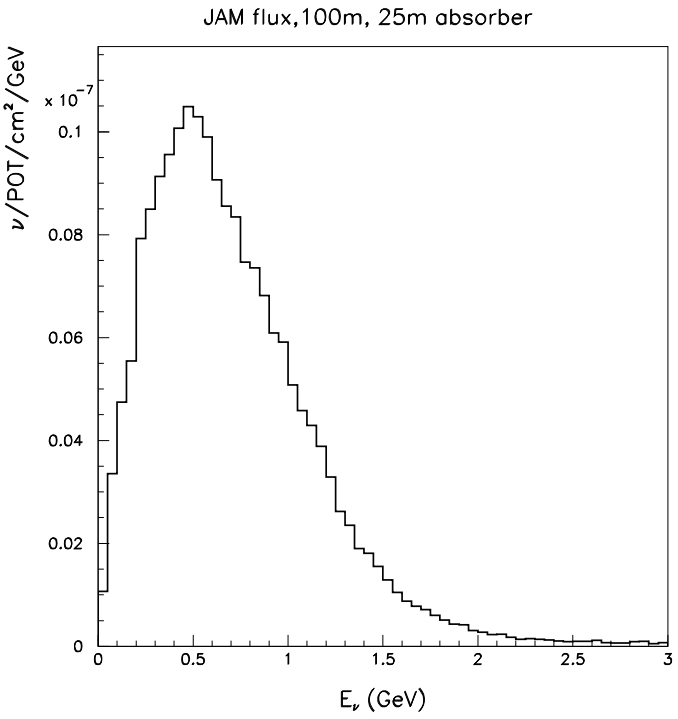

Figure 4: Calculated $\nu_m u$ flux at a 100m location on the booster neutrino beamline.

3 Neutrino Scattering Physics using the Main Injector with a Fermilab Proton Driver

3.1 Introduction

As indicated, at the time of startup for a Fermilab Proton Driver (FPD), the MINERνA experiment [4] will have completed running parasitically to the MINOS experiment. A brief summary of the MINERνA physics program indicates that the major topics of ν - nucleus scattering physics will have been well-covered.

3.1.1 Low-energy Neutrino Cross-sections: Quasi-elastic Scattering

As shown in Figure 5, MINERνA will have measured the cross-section up to E_ν = 20 GeV with statistical uncertainties ranging from $\leq$ 1% at low E_ν up to 7% at E_ν = 20 GeV. The expected beam systematic uncertainty is 4–6% thanks to precision measurements of hadron production (the largest uncertainty in predicting neutrino flux) by the current MIPP experiment [11].

For the axial-vector form-factor, measurement of neutrino quasi-elastic scattering is the most direct way to improve our knowledge. MINERνA's ability to measure $d\sigma/dQ^2$ to high Q^2 will have allowed investigation of the non-dipole component of the axial-vector form factor to an unprecedented accuracy. Figure 5 shows the extraction of the axial-vector form factor from the quasi-elastic event sample accumulated over a 4-year MINERνA run. The data points are plotted as a ratio of F_A/F_A(Dipole) with the indicated assumptions. Also shown are the currently available values of F_A from early experiments. MINERνA will have measured the axial nucleon form-factor with precision comparable to vector form-factor measurements at JLab. Combining MINERνA's measurements with Jefferson Lab data that will be available by the time of the FPD will permit precision extraction of all form factors needed to improve and test models of the nucleon [12].

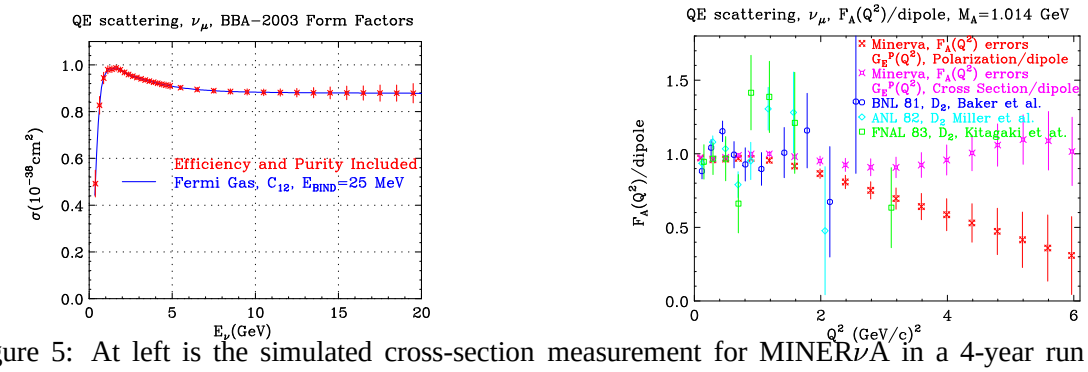

Figure 5: At left is the simulated cross-section measurement for MINERνA in a 4-year run (statistical errors only) assuming M_A=1.00 GeV and the Fermi gas model. At right are the projected axial form-factor results for MINERνA for two different assumptions: F_A/dipole=G_E^p/dipole from cross-section and F_A/dipole=G_E^p/dipole from polarization. Also shown are the extracted values of $F_A(q^2)$/dipole for deuterium bubble chamber experiments Baker *et al.* [13], Kitagaki *et al.* [14] and Miller *et al.* [15].

3.1.2 Low-energy Neutrino Cross-sections: Resonance Production

To simulate resonance-mediated reactions, Monte-Carlo programs still use early theoretical predictions by Rein & Sehgal [16] or results from electro-production experiments, since existing data on neutrino-induced resonance production is inadequate. The theoretical and experimental picture of the resonance and transition regions is far more obscure than the quasi-elastic and DIS regions which border it.

Analysis of resonance production in MINERνA [17] will have focused on several experimental channels, including inclusive scattering in the resonance region ($W < 2$ GeV) and exclusive charged and neutral pion production.

This channel may need additional investigation with an even-more fine-grained detector such as a LAr TPC. The investigation of this channel is not limited by beam intensity but rather by detector techniques.

3.1.3 Low-energy Neutrino Cross-sections: Coherent Pion Production

MINERνA, with its high statistics and variety of nuclear targets, will have greatly improved our experimental understanding of coherent processes. Figure 6 shows the estimated statistical precision of MINERνA's CC coherent scattering measurement, as a function of neutrino energy, after background subtraction. The model of Rein & Seghal [18] has been assumed. Also plotted are the only currently available measurements in this kinematic region showing their total errors.

MINERνA's CC coherent event sample will also have been used to study the differential cross-sections. Comparison of the overall rates of NC and CC production, as well as the pion energy and angular distributions will allow valuable tests of the various models. For several recent models, the predicted NC/CC ratios in coherent scattering differ by around 20% [18, 8].

MINERνA will also have compared the reaction rates for lead, iron and carbon. The A dependence of the cross-section depends mainly on the assumed model of the hadron–nucleus interaction and serves as a crucial test for that component of the predictions [20]. Figure 6 illustrates the broad range in A covered by MINERνA's measurement of the coherent pion cross-section. The shaded band is the range in A covered by existing experiments.

The MINERνA results [19] will have eliminated several models for coherent production by the time a FPD comes on-line.

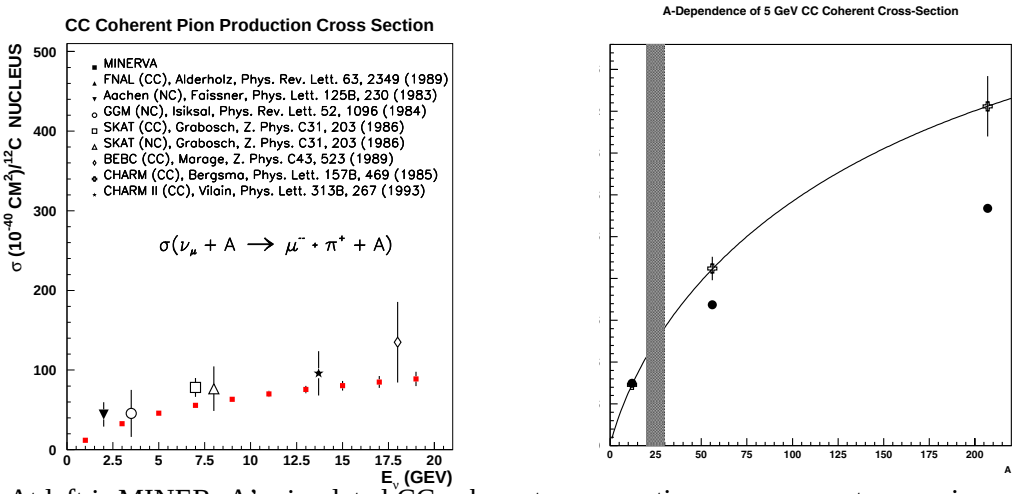

Figure 6: At left is MINERνA's simulated CC coherent cross-section measurement, assuming a 4-year run, statistical errors only, compared with published data. At right, the range of A-dependence in coherent pion-production accessible to MINERνA is compared to the narrow range of existing data, shown by the shaded band. The curve is the prediction of the Rein-Seghal model [18] while the solid circles correspond to the prediction of Paschos and Kartavtsev [8]

3.1.4 Nuclear Effects in Neutrino Scattering

Analysis of neutrino reactions with nuclear media requires understanding the nuclear environment's effect on the process [22]. There are two general categories of such nuclear effects:

- The neutrino interaction probability on nuclei is modified relative to free nucleons. Nuclear effects of this type have been extensively studied in DIS structure function measurements using muon and electron beams, but have not been explored with neutrinos. Depending on the kinematic region, these nuclear effects can be quite different for neutrinos, particularly the shadowing phenomenon [21].

- Hadrons produced in a nuclear target may undergo final-state interactions (FSI), including re-scattering and absorption. These effects may significantly alter the observed final-state configuration and measured energy [25, 26], and are sizable at neutrino energies typical of current and planned oscillation experiments [23].

The hadron shower observed in neutrino experiments is actually the *convolution* of these two effects. FSI effects are dependent on the specific final states that, even for free protons, differ for neutrino and charged-lepton reactions. The suppression or enhancement of particular final states by nuclear effects also differ for neutrino and charged lepton reactions. For these reasons, measurements of nuclear effects with charged leptons cannot be simply applied to neutrino-nucleus interactions.

It has recently been suggested that, for a given Q^2, shadowing can occur at much lower energy transfer (ν) for neutrinos than for charged leptons. This effect is unaccounted for in neutrino event generators. As explained in [24], for a given Q^2 the cross-section suppression due to shadowing occurs for much lower energy transfer (ν) in neutrino interactions than for charged leptons. Figure 7 shows the predicted difference between neutrino and charged lepton shadowing as a function of the energy transfer (ν). On the left is the ratio of iron to deuterium while on the right is shown the ratio of lead to carbon. The projected statistical error on the ratio of lead to carbon is order 2% at ν = 6 GeV. Clearly this is an important effect, and without MINERνA, there are no data available to measure it.

MINERνA will have carefully studied these effects with targets of carbon, iron and lead [24]. What will be missing is a comparison with deuterium which is essential for maximal understanding of these effects.

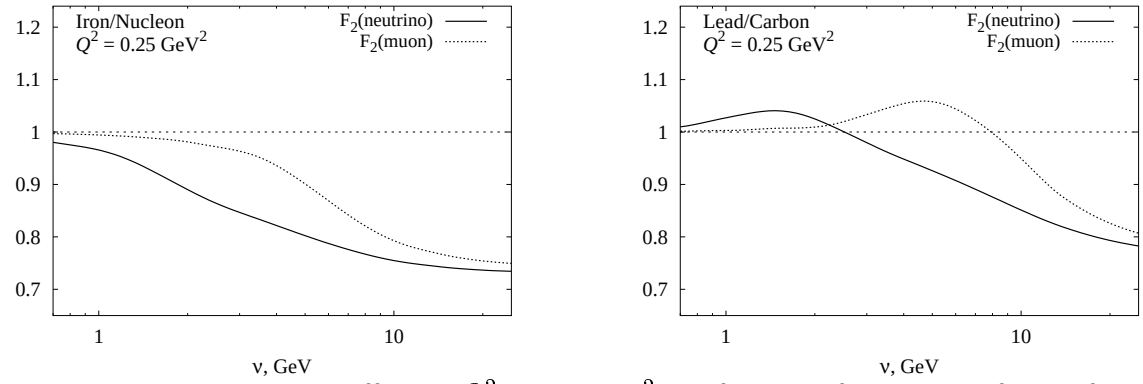

Figure 7: Predicted shadowing effects at Q^2 = 0.25 GeV^2 as a function of energy transfer (ν), for neutrinos (solid line) and muons (dotted line). The plot on the left is for iron compared to deuterium while the right plot is lead compared to carbon, which is what MINERνA will measure.

3.1.5 The Perturbative - Non-Perturbative Interface and Deep-Inelastic Scattering

Despite the apparent dichotomy between the partonic and hadronic regimes, in nature there exist instances where the low-energy behavior of cross-sections (averaged over appropriate energy intervals) closely resembles that at asymptotically high energies, calculated in terms of quark-gluon degrees of freedom. This phenomenon is referred to as *quark-hadron duality* and is the focus of substantial recent interest in probing the structure of the nucleon [41, 42, 39, 28, 29]. For example, there are over 10 related experiments at JLab.

Understanding this transition requires reliable data in three kinematic regimes: in the scaling domain of high Q^2 DIS scattering; in the hadronic region of resonances and quasi-elastic scattering; and, perhaps most importantly, in the moderate Q^2 region between the two, where the transition is most dramatically manifested. MINERνA will have addressed this compelling topic for the first time with neutrinos with measurements spanning all three regimes, providing reliable data in the crucial transition region [30].

3.2 Goals of a MI Neutrino Scattering Physics Program in the Proton Driver Era

As shown, low-to-medium energy ν- **nucleus** scattering will be quite well covered. However $\overline{\nu}$- **nucleus** and ν / $\overline{\nu}$ - **nucleon**, in this same important energy range, will still not have been covered as needed. The simple reason why these topics will not have been covered is the meager event rate associated with them. The $\overline{\nu}$ event rate is down a factor of (3 - 5), depending on energy range, compared to the ν rate. This comes from a combination of the cross-section ratio and the production rate ratio of π^+ to π^-. Combining this factor with the low absolute cross-section associated with low-energy neutrinos, as with the NuMI - le beam configuration, and what would take a 3 year run to accumulate with ν would take 9 - 15 years with $\overline{\nu}$. Similarly a neutrino scattering physics program on the nucleon (Liquid H_2 and D_2 targets) has an event rate an order-of-magnitude lower than with a carbon target. To completely understand ν / $\overline{\nu}$ - **nucleon** as well as $\overline{\nu}$- **nucleus** scattering physics, the higher statistics available with a FPD is essential.

3.2.1 Neutrino Beam Requirements

The NuMI neutrino beam will need modifications to run in the FPD era to accommodate the increased instantaneous intensity on the target. However, the standard 2-horn beam provides a very pure ν beam with only a small admixture of $\overline{\nu}$ background. Unfortunately, the converse is not true. The NuMI 2-horn $\overline{\nu}$ le-beam actually yields **more** ν events than $\overline{\nu}$ events. This is due to the forward going higher energy positive pions that go right through the neck of the horns and, thus experience no deflecting magnetic field. For a high-precision $\overline{\nu}$ beam in the FPD era the logical choice of beam would be a sign-selected beam such as was used by Fermilab experiment E-815 (NuTeV) [31] and described by R. Burnstein at the Proton Driver

Workshop. With this sign-selected beam, the ν contamination of the $\overline{\nu}$ beam is reduced to 4x10^{-3}, a dramatic improvement compared to the 2-horn beam.

3.2.2 Detector Requirements

An important goal of an FPD neutrino scattering program will be careful study of ν / $\overline{\nu}$ - nucleon scattering. This will require a large liquid hydrogen/deuterium target. With the NuMI he-beam running with a FPD, a fiducial volume of radius = 80 cm and length = 150 cm would collect 1.8 M events on hydrogen and nearly 4 M events on deuterium for 1.25 x 10^{21} POT - roughly a year of FPD running. The challenge will be to know what is happening to the events produced within the hydrogen/deuterium target before they leave the target and enter the tracking detectors surrounding the target. A way to record the tracks within the cryogenic liquid target is make the target active as in a Bubble Chamber. Contemporary large bubble chambers are being developed for WIMP searches by a University of Chicago/Fermilab collaboration and for Bubble Chamber spectroscopy by Los Alamos lab. These new chambers use CCD coupled readout to directly transfer the image to disk. Patern recognition and tracking software developed for emulsion experiments can then be directly employed to reproduce the three-dimensional images.

4 Nuclear Physics Interest

4.1 Introduction

Over the past 20 years the field of "nuclear physics" has come to encompass many areas of subatomic physics outside its traditional domain. The historical core of the field, the study of nuclear structure remains, has continued to flourish and expand into the regime of highly excited nuclei and nuclei far from stability. However, new areas of interest have come to form a large part of the current endeavors. The most recent accelerators built for nuclear physics studies, the Relativistic Heavy Ion Collider (RHIC) and the Continuous Electron Beam Accelerator Facility (CEBAF) at the Thomas Jefferson National Accelerator Facility (JLab), have as their emphasis the study of physics which has little to do with traditional nuclear physics. RHIC was primarily built to search for the quark-gluon plasma and much of the work at JLab deals with the structure of the nucleon and nucleon resonance physics. The physics studied at JLab has much in common with the traditional interests of high energy physics. There are many topics being actively studied at JLab, or planned for study after the JLab upgrade to 12 GeV, with electron and photon probes in the "intermediate energy" range (roughly 1-10 GeV) which were initially investigated by high energy physicists. The high quality beams at JLab have made renewed studies a fruitful endeavor. For many topics neutrinos would be an ideal probe if neutrino beams of sufficient quality could be produced. In the following sections we will review those topics and outline what improvements in neutrino facilities be required to interest members of the nuclear physics community in the Proton-Driver program.

4.2 Elastic Form Factors

The description of the nucleon requires measurement of the internal structure (the parton distribution functions) and those parameters which describe the behavior of the nucleus as a whole - the elastic form factors. There are two electromagnetic form factors of the nucleon. Although there are many (infinite, in fact) ways to parameterize the nucleon form factors, the most intuitive way is in terms of the electric G_E and magnetic G_M form factors. At least for low momentum transfer and in the Breit frame, these can be related to the distribution of charge and magnetism in the nucleus. For many years the elastic form factors were considered to be known quantities. Textbooks reported that they were well described by the "dipole" form. The dipole form was attractive in that it corresponds to the reasonable assumption that the charge and magnetic distributions were exponential. Although early measurements [32] seemed to confirm the dipole distributions,

precision measurements at JLab [33, 34] showed that the electric form factor had a distinctly different form. As shown in Fig. 8 the electric form factor drops more quickly than the magnetic form factor, indicating that the charge distribution has a broader spatial distribution than the distribution of magnetism.

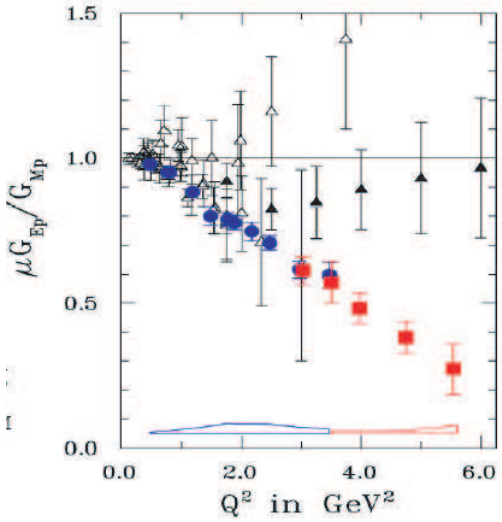

Figure 8: Ratio of the electric to magnetic form factor measured using polarization transfer. Data taken from Ref. [34].

The different behavior of the two form factors takes on a greater significance when expressed in terms of the Dirac and Sachs form factors F_1 and F_2. Perturbative QCD predicts that the ratio Q^2F_1/F_2 should be constant. Instead it appears QF_1/F_2 approaches a constant. Although the reason for this is not completely understood, it does appear that it is an indication of orbital angular momentum of the quarks.

So, to the surprise of everyone, the measurement of the elastic form factors gave one of the most unexpected results from JLab. The nucleon also has weak form factor which has always been assumed to have a dipole distribution as well. However, the statistical precision of existing measurements is poor and the Q^2 range too limited to make any definitive statement on the form. This can be measured through parity violation in electron-nucleon scattering, with limited precision. Neutrino-nucleon elastic (or quasi-elastic) scattering depends on both the electromagnetic form factors and the weak form factor. Nearly half the cross section is due to the weak form factor, making neutrino-nucleon scattering an ideal probe of the weak form factor.

Planned measurements of the weak form factor (e.g. the MINERνA experiment) use scattering from nucleons in nuclei. Although the statistical precision will be reasonably good, there is an uncertainty in both extracting the form factor from scattering from a bound nucleon due to final state interactions and other conventional effects, as well as the possibility of modification of the form factor by the nuclear medium. JLab and Mainz measurements of the form factor in the ^{4}He have in fact shown indications of a significant (several percent) effect [35, 36]. Thus, measurement of the proton form factor using hydrogen and of the neutron form factor using deuterium, is essential.

4.3 Parton Distribution Functions

One of the most significant discoveries of very high energy scattering of electrons and muons from nucleons is the confirmation of the existence of partons. The key to understanding the basic substructure of the nucleon is measurement of the parton distribution functions. The cross section for high energy scattering has been found to be a function of x only, a property called scaling. Numerous measurements have been

made using electron and muon deep inelastic scattering (DIS) and other processes such as the Drell-Yan production. Scattering of electrons and muons always involves combinations of the valence quarks and sea quarks. Separation of the valence and sea quark distributions is only possible using neutrinos because they have the required sensitivity to flavor that is absent in other probes. The neutrino structure functions F_1, F_2, and F_3 are given by:

$$F_2^{\nu,\bar{\nu}} = 2xF_1^{\nu,\bar{\nu}} = 2x\sum_q c_q^{\nu,\bar{\nu}} q(x,Q^2)$$

where $c_q^{\nu} = 1$ for $q = d, s, \bar{u}, \bar{c}$ and $c_q = 0$ for $q = u, c, \bar{d}, \bar{s}$, and vice versa for $\bar{\nu}$.

$$F_3^{\nu,\bar{\nu}} = 2\sum_q \tilde{c}_q^{\nu,\bar{\nu}} q(x,Q^2)$$

where $\tilde{c}_q^{\nu} = 1$ for $q = d, s$ and -1 for $q = \bar{u}, \bar{c}$, etc.

Thus, precision measurements of structure functions using both neutrinos and anti-neutrinos allows determination of $q - \bar{q}$. There are still many questions open on the parton distributions. For example, although we know that the net number of strange quarks is zero, there is no reason for $s(x) = \bar{s}(x)$. In fact, a global analysis to determine the strange sea asymmetry as a function of x shows moderate deviations from zero at higher Q^2. Differences between s and $\bar{s}$ can also have a significant impact on the extraction of $\sin^2\theta_W$ from $\nu, \bar{\nu}$ data [37].

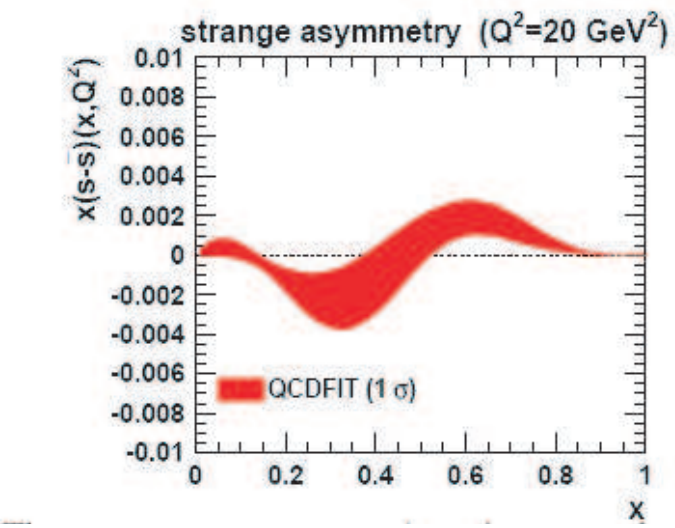

Figure 9: The strange sea asymmetry (on sigma error band) as obtained from a global fit of all data from Ref. [37].

Even the valence PDF's are not well known at large x. The ratio of d/u is normally determined by comparing scattering from the proton and neutron. However, because no free neutron target exists, the deuteron is used as a neutron target. Although this makes little difference in the extracted value at small x, uncertainties in the nuclear corrections become substantial at for x larger than about 0.6, and make determination of the ratio essentially impossible for x larger than about 0.8, as shown in Fig. 10. The ratio of d/u can be determined without any nuclear structure effect corrections by using neutrino and antineutrino scattering on hydrogen, as the ratio $F_2^{\nu p}/F_2^{\bar{\nu} p}$ is equal to d/u.

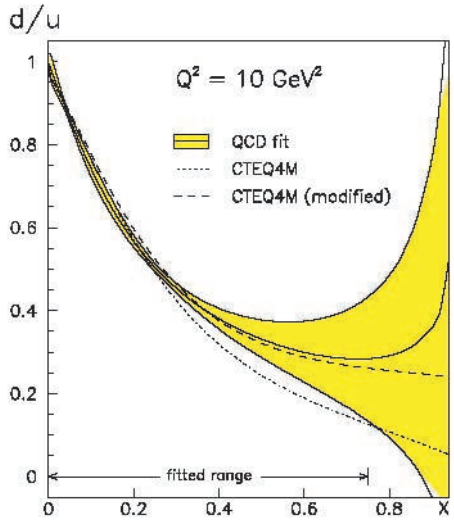

Figure 10: The d/u ratio showing the uncertainty due to nuclear effects in the deuteron. Figure taken from Ref. [38].

4.4 Strange Quarks in the Nucleon

Although the nucleon is made up of only u and d valence quarks, it is well known that the sea quarks must have a significant component of strange and anti-strange quarks. Determination of the strange quark contribution to the nucleon form factors has been a major component of the JLab program. The only access to the strange quark using electron scattering is via parity violation. However, it appears that parity violation experiments are likely to be able only to put upper limits on the strange quark content of the nucleon.

Obtaining significantly better measurements of the strange quark content than achieved by parity violation experiments requires measurements using neutrinos. The ideal measurement would be measurement of the ratio $(\nu p \rightarrow \nu p)/(\nu n \rightarrow \mu p)$ on a deuterium target. Because this requires measurement of a neutral current on a liquid target, a narrow band neutrino beam of high intensity is required.

4.5 Duality

Although all evidence to date is that QCD is the correct theory of strong interactions, there are many features of QCD that we do not yet fully understand. In particular, we have a very poor understanding of the details of the transition from the region where quarks and gluons are the appropriate degrees of freedom to the region best described using baryons and mesons.

Scattering is best understood in the high Q^2 region where the reaction is understood in terms of perturbative QCD. The simple scaling behavior of the structure functions discovered in DIS is clear evidence of the primary mechanism is the scattering from partons.

In the region of modest Q^2 (1-10 GeV^2) the scattering of electrons is dominated by resonance production. Scattering of electrons in the resonance region can also be described with the same formalism as DIS. However, there is no obvious reason to expect the structure functions measured there should be related to the DIS values, since the scattering is from correlated partons forming the nucleon. Despite this, many instances have been found where the DIS and resonance scattering are closely correlated. For example, experiments at JLab [39] have found that the F_2 structure function measured in the resonance region closely follows that measured in the DIS region, as show in Fig. 11. The phenomenon, called quark-hadron duality, has also been observed in other processes, such as e^+e^- annihilation into hadrons.

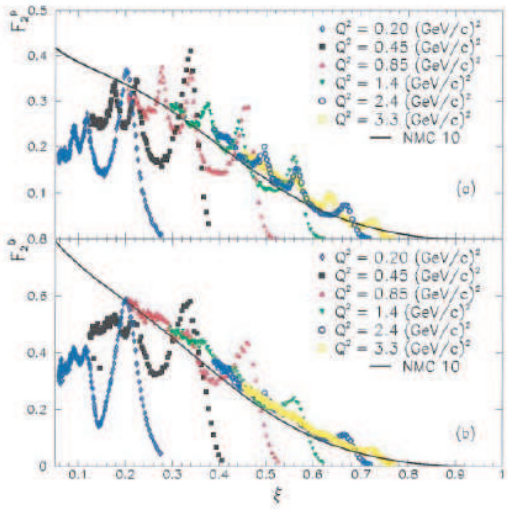

Figure 11: Structure functions measured in the resonance region at JLab on hydrogen and deuterium targets. Figure taken from Ref. [39]

The origins of duality are not well understood [40, 41, 42, 43, 44, 45, 46]. Although it is expected that duality should also exist for weak interactions, the data at present are not of sufficient quality to make any clear determination of its validity. The next decade of experiments, especially with MINERνA, should provide some information on the validity of duality using neutrinos. However, high precision measurements using anti-neutrinos and nucleon (hydrogen and deuterium) targets will be required in order to fully explore the origins of duality.

4.6 Generalized Parton Distribution Functions

One of the most exciting developments in the theory of the structure of the nucleon has been the understanding of generalized parton distributions [47, 48, 49, 50, 51]. The usual PDF's are sensitive only to the longitudinal momentum distributions of the parton. In contrast, the elastic form factors integrate over the longitudinal distributions of the partons and describe the spatial distribution. Ji and Radyushkin, in particular, developed a formalism which gives a complete picture of the nucleon in which the spatial distribution as a function of the longitudinal momentum distribution can be determined. Measurement of the GPD's will allow a complete 3-dimensional picture of the nucleon to be obtained. The GPD's are difficult to access experimentally because they require measurement of exclusive final states. The most promising reaction to date is deep virtual Compton scattering (DVCS), i.e. $p(e, e'\gamma p)$. Measurements are currently either underway or planned at JLab to measure the GPD's using the DVCS reaction.

However, a complete determination of the GPD's requires flavor separation which can only be accomplished using neutrinos and anti-neutrinos. Because of the requirement that exclusive final states be measured, the reaction is difficult to perform on nuclei. Although MINERνAwill measure GPD's on carbon, this is considerably inferior to measurement on the proton. A true GPD measurement would require measurement of the $p(\bar{\nu}, \mu\gamma n)$ reaction using a free proton (i.e. hydrogen) target or $n(\nu, \mu\gamma p)$ reaction using a free neutron target (in practice, a deuteron target). Estimates for this "weak DVCS" process are currently being made by A. Psaker [52]. The CC cross section is of order 10^{-41}cm^2 and the NC about 10 times smaller. These small cross sections will clearly require higher intensity neutrino beams than are available at NuMI if measurements on hydrogen are to be performed.

4.7 Role of Proton Driver for Nuclear Physics

During the coming years we anticipate MINERνA and other experiments will make extensive measurements of charged current (CC) ν-nucleus scattering and it is unlikely that the increased intensity will be able to make significant improvements of those measurements. What will be missing are precision CC $\bar{\nu}$-nucleus measurements, neutral current (NC) $\nu, \bar{\nu}$-nucleus measurements, and most importantly, $\nu, \bar{\nu} - p, n$ measurements for both NC and CC. Of course, the closest we can get to a free neutron target is deuterium, but that is not peculiar to neutrinos.

CC measurements are (relatively) easily made with both neutrinos and anti-neutrinos because the sign of the outgoing muon identifies the type of neutrino and the momentum of the neutrino can be measured with reasonable precision. However, NC measurements require both high precision measurement of the outgoing products and knowledge of the incident neutrino type. The NuMI anti-neutrino beam has a high contamination ($\tilde{5}0\%$) of neutrinos, making NC measurements rather difficult. High statistics and high precision measurements using anti-neutrinos will require nearly pure anti-neutrino beams.

The NuMI beam will give rates of around 2000 events/year/ton/GeV for CC and neutrino beams. The cross section for anti-neutrinos is only about a third of this and the antineutrino beam intensity is only about a third of the neutrino intensity. The rates are then only a few hundred/year/ton/GeV. Making a pure anti-neutrino beam will reduce this intensity by a factor of five or so, reducing anti-neutrino beams to a level unable to give a statistically significant result for any of the quantities of interest.

The proton driver will provide a primary $\nu, \bar{\nu}$ 5-10 times greater than NuMI. This would allow pure $\bar{\nu}$ beams of comparable intensity to the current neutrino beams. With these intensities many of the measurements described above should be within reach.

References

[1] A. Suzuki *et al.*, Nucl. Instr. Meth. **A453**, 165 (2000); T. Ishii *et al.*, Nucl. Instr. Meth. **A482**, 244 (2002).

[2] E. Church *et al.*, FERMILAB-P-0898 (1997); `http://library.fnal.gov/archive/test-proposal/0000/fermilab-proposal-0898.shtml`.

[3] T2K experiment, `http://www-nu.kek.jp/jhfnu/index_e.htm l`.

[4] D. Drakoulakos *et al.* [Minerva Collaboration], "Proposal to perform a high-statistics neutrino scattering experiment using a fine-grained detector in the NuMI beam," arXiv:hep-ex/0405002. `http://www.pas.rochester.edu/minerva/`.

[5] FINeSSE experiment, `http://www-finesse.fnal.gov/index.h tml`.

[6] B. W. Filippone and X. D. Ji, Adv. Nucl. Phys. **26**, 1 (2001), hep-ph/0101224.

[7] L. A. Ahrens *et al.*, Phys. Rev. **D35**, 785 (1987).

[8] E. A. Paschos and A. V. Kartavtsev, arXiv:hep-ph/0309148 (2003).

[9] R. Shrock, Phys. Rev. **D12**, 2049 (1975), A. A. Amer, Phys. Rev. **D18**, 2290 (1978).

[10] L. B. Auerbach *et al.*, Phys. Rev. D **63**, 112001 (2001) [hep-ex/0101039].

[11] Y. Fisyak *et al.* [The MIPP Collaboration], "P-907: Proposal to Measure Particle Production in the Meson Area Using Main Injector Primary and Secondary Beams", proposal to the FNAL PAC, May 2000. R. Raja *et al.* [The MIPP Collaboration], "Addendum to the P-907 Proposal", proposal to the FNAL PAC, October 2001. `http://ppd.fnal.gov/experiments/e907/e907.htm`

[12] A. Bodek, H. Budd, "Quasi-Elastic Scattering", MINERνA Note 100, September, 2004. http://www.pas.rochester.edu/minerva/

[13] N. J. Baker *et al.,* Phys. Rev. **D23**, 2499 (1981).

[14] T. Kitagaki *et al.,* Phys. Rev. **D26**, 436 (1983).

[15] K.L. Miller *et al.,* Phys. Rev. D26 (1982) 537.

[16] D. Rein and L. M. Sehgal, Annals Phys. **133**, 79 (1981).

[17] O. Lalakulich, E. Paschos, S. Wood. "The Study of Resonance Production in the MINERνA Experiment", MINERνA Note 200, September, 2004. http://www.pas.rochester.edu/minerva/

[18] D. Rein and L. M. Sehgal, Nucl. Phys. **B223**, 29 (1983).

[19] H. Gallagher, D. Harris, A. Kartavtsev, and E. Paschos, "Neutral and Charged Current Neutrino-Nucleus Coherent Measurements", MINERνA Note 300, October, 2004. http://www.pas.rochester.edu/minerva/

[20] E. Paschos and A. Kartavtsev (private communication).

[21] B.Z. Kopeliovich, hep-ph/0409079.

[22] MINERνA Collaboration, *op. cit.*, pgs. 99 - 108, 192 - 200.

[23] E. A. Paschos, M. Sakuda, I. Schienbein and J. Y. Yu, arXiv:hep-ph/0408185, (2004).

[24] S. Boyd, S. Kulagin, J. G. Morfin and R. Ransome, "Studying Neutrino-induced Nuclear Effects with the MINERνA Detector". MINERνA Note 700, September, 2004. http://www.pas.rochester.edu/minerva/

[25] M.K. Jones *et al.,* Phys. Rev. **C48**, 2800 (1993); R.D. Ransome *et al.*, Phys. Rev. **C46**, 273 (1992); R.D. Ransome *et al.*, Phys. Rev. **C45**, R509 (1992).

[26] D. Rowntree *et al.,* Phys. Rev. **C60**, 054610 (1999); B. Kotlinksi *et al.*, Eur. Phys. J. **A9**, 537 (2000).

[27] MINERνA Collaboration, *op. cit.*, pgs. 83 - 94.

[28] I. Niculescu *et al.*, Phys. Rev. Lett. **85** (2000) 1186.

[29] R. Ent, W Melnitchouk, and C .E. Keppel, "Quark-Hadron Duality in Electron Scattering", submitted to Physics Reports.

[30] C. E. Keppel and I. Niculescu. "Studying the Perturbative / Non-Perturbative QCD Interface with the MINERνA Detector". MINERνA Note 500, September, 2004. http://www.pas.rochester.edu/minerva/

[31] M. H. Shaevitz, S. R. Mishra, F. Sciulli, R. H. Bernstein, F. Borcherding, M. Lamm and F. Taylor, FERMILAB-PROPOSAL-0815, FNAL-TM 1884

[32] L. Andivahis *et al.*, Phys. Rev. D **50**, 5491 (1994).

[33] M. K. Jones *et al.*, Phys. Rev. Lett **84**, 1398 (2000).

[34] O. Gayou *et al.*, Phys. Rev. Lett **88**, 092301 (2002) .

[35] S. Dieterich *et al.* Phys. Lett. B **500**, 47 (2001).

[36] S. Strauch *et al.* Phys. Rev. Lett. **91**, 052301 (2003).

[37] B. Portheault, hep-ph/0406226 (2004).

[38] M. Botje, Eur. Phys. J. C **14**, 285 (2000).

[39] I. Niculescu *et al.*, Phys. Rev. Lett. **85**, 1182-1185 (2000).

[40] W. Melnitchouk, R. Ent, C.E. Keppel, accepted by Physics Reports.

[41] Sabine Jeschonnek and J.W. Van Orden, Phys. Rev. D **69**, 054006 (2004).

[42] F. E. Close and Nathan Isgur, Phys. Lett. B **509**, 81-86 (2001).

[43] R. Ent, C. E. Keppel, I. Niculescu, PRD **62**, 073008 (2000).

[44] C.E. Carlson and N.C. Mukhopadhyay, Phys. Rev. D **47**, 1737 (1993).

[45] M. Diemoz, F. Ferroni, and E. Longo, Phys. Rev. **130**, 293 (1986).

[46] R. Belusevic and D. Rein, Phys. Rev. D **38**, 2753 (1988); Phys. Rev. D **46**, 3747 (1992).

[47] X. Ji, Phys. Rev. Lett. **78**, 610 (1997).

[48] X. Ji, Phys. Rev. **D55**, 7114 (1997).

[49] A. V. Radyushkin, Phys. Lett. **B380**, 417 (1996).

[50] A. V. Radyushkin, Phys. Lett. **B385**, 333 (1996).

[51] J.C. Collins, L. Frankfurt, and M. Strikman, Phys. Rev. **D56**, 2982 (1997).

[52] private communcation.